Particle Identification using the Time-over-Threshold Method in the ATLAS Transition Radiation Tracker

T. Akesson [a] E. Arik [b] K. Assamagan [c] K. Baker [c] E. Barberio [d] D. Barberis [d,p] H. Bertelsen [e] V. Bytchkov [f] J. Callahan [g] A. Catinaccio [d] H. Danielsson [d] F. Dittus [d] B. Dolgoshein [h] N. Dressnandt [i] W. L. Ebenstein [j] P. Eerola [a] P. Farthouat [d] D. Froidevaux [d] Y. Grichkevitch [k] Z. Hajduk [l] J. R. Hansen [e] P. T. Keener [i] G. Kekelidze [f] S. Konovalov [m] T. Kowalski [n] V. A. Kramarenko [k] A. Krivchitch [o] A. Laritchev [k] P. Lichard [d] A. Lucotte [d] B. Lundberg [a] F. Luehring [g] E. Mailov [b] A. Manara [g] K. McFarlane [c] V. A. Mitsou [d,q] S. Morozov [h] S. Muraviev [m] A. Nadtochy [o] F. M. Newcomer [i] J. Olszowska [l] H. Ogren [g] S. H. Oh [j] V. Peshekhonov [f] C. Rembser [d] A. Romaniouk [h,d] D. Rousseau [d,r] D. R. Rust [g] V. Schegelsky [o] M. Sapinski [l] A. Shmeleva [m] S. Smirnov [h] L. N. Smirnova [k] V. Sosnovtsev [h] S. Soutchkov [h] E. Spiridenkov [o] V. Tikhomirov [m] R. Van Berg [i] V. Vassilakopoulos [j] C. Wang [j] H. H. Williams [i]

[a] *Fysiska Institutionen, Lunds Universitet, Lund, Sweden*

[b] *Bogazici University, Department of Physics, Istanbul, Turkey*

[c] *Hampton University, Hampton, Virginia, 23668 USA*

[d] *European Laboratory for Particle Physics (CERN), Geneva, Switzerland*

[e] *Nils Bohr Institute, University of Copenhagen, Copenhagen, Denmark*

[f] *Joint Institute of Nuclear Research, Dubna, Russia*

[g] *Indiana University, Bloomington, Indiana, USA*

[h] *Moscow Engineering and Physics Institute, Moscow, Russia*

[i] *Department of Physics and Astronomy, University of Pennsylvania, Philadelphia, Pennsylvania, USA*

[j] *Physics Department, Duke University, Durham, North Carolina, USA*

[k] *Moscow State University, Institute of Nuclear Physics, Moscow, Russia*

[l] *Henryk Niewodniczanski Institute of Nuclear Physics, Cracow, Poland*

[m] *P. N. Lebedev Institute of Physics, Moscow, Russia*

[n] *Faculty of Physics and Nuclear Techniques of the Academy of Mining and Metallurgy, Cracow, Poland*

[o] *Petersburg Nuclear Physics Institute, Gatchina, St. Petersburg, Russia*

[p] *also at University of Genova, Genova, Italy*

[q] *also at University of Athens, Physics Department, Athens, Greece*

[r] *now at Laboratoire de l'Accélérateur Linéaire, Orsay, France*

Abstract

Test-beam studies of the ATLAS Transition Radiation Tracker (TRT) straw tube performance in terms of electron-pion separation using a time-over-threshold method are described. The test-beam data are compared with Monte Carlo simulations of charged particles passing through the straw tubes of the TRT. For energies below 10 GeV, the time-over-threshold method combined with the standard transition-radiation cluster-counting technique significantly improves the electron-pion separation in the TRT. The use of the time-over-threshold information also provides some kaon-pion separation, thereby significantly enhancing the B-physics capabilities of the ATLAS detector.

Key words: Time-over-threshold. Straw. Particle identification.

[1] Contact person H. Ogren
E-mail: ogren@indiana.edu

1 Introduction

The Transition Radiation Tracker (TRT) [1] is a part of the Inner Detector of the ATLAS experiment. It is designed to provide powerful pattern recognition capabilities and electron identification via transition radiation.

The TRT is a straw drift-tube detector, with a central barrel section and two end-cap sides, giving an average of 35 crossed straws per track. In the barrel TRT, axial straws are embedded in fibre radiators, while, in the end-caps, layers of radial straws and foil radiators are alternated. These geometries have been chosen in order to have an approximately constant number of straws crossed by charged particles with $p_{\mathrm{T}} > 0.5\,\mathrm{GeV}$ over the full rapidity coverage ($|\eta| < 2.5$). Transition radiation is produced when a charged ultra-relativistic particle crosses the interface between different media, mainly polypropylene (fibres or foils) and air in the case of the TRT. The transition-radiation photons are emitted at very small angle with respect to the parent-particle trajectory and are therefore most often detected in the same straws as those crossed by the parent particle.

The TRT straw drift-tubes provide two types of information: the distance of closest approach of the track to the anode wire (for tracking purposes via drift-time measurements) and the energy deposited in the straw (for particle identification). This energy deposition is the sum of the ionisation losses of the charged particle crossing the straw and of the usually larger energy depositions due to transition-radiation photon absorption.

The low-threshold discriminator level is set to a nominal value of 200 eV, which is safely above the noise level ($\sigma \sim 40\,\mathrm{eV}$) and significantly below the average energy loss of $\sim 2\,\mathrm{keV}$, expected for minimum-ionising particles traversing the straw gas. With this low-threshold setting, the front-end electronics detects the initial ionisation cluster for precise drift-time determination.

The high-threshold discriminator level is set to a nominal value of 5 keV, which is optimised for e/π separation. Particle identification studies based on the cluster-counting technique with different TRT prototypes have been reported in [2–4]. In these studies, e/π separation was achieved by counting the number of high-threshold hits along the reconstructed track. For electrons, the tail above 5 keV is dominated by transition-radiation hits, while for pions it is mostly due to δ-rays. By requiring more than a certain number of high-threshold hits along the track, the probability to misidentify pions as electrons was measured as a function of the electron efficiency. This procedure is illustrated in Fig. 1, where a display of a simulated $\mathrm{B}^0_{\mathrm{d}} \to \mathrm{J}/\psi\mathrm{K}^0_{\mathrm{s}}$ event (at the low luminosity nominal value of $10^{33} cm^{-2} s^{-1}$) in the ATLAS barrel TRT is shown, and in Fig. 2, where portions of a pion track from the $\mathrm{K}^0_{\mathrm{s}}$ decay and of an electron track from a J/ψ decay are shown in an enlarged frame (see box in Fig. 1). Dots represent straws crossed by charged particles. Electron tracks contain many more high-threshold hits (larger points) than pion tracks.

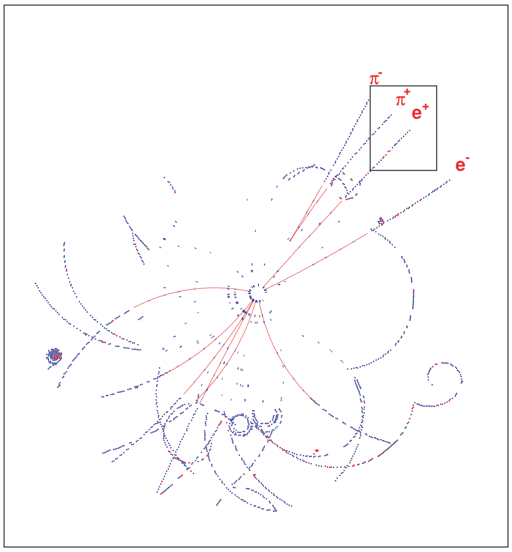

Fig. 1. Display of a simulated $B_d^0 \to J/\psi K_s^0$ event in the ATLAS barrel TRT, at low luminosity ($10^{33} cm^{-2} s^{-1}$). Reconstructed tracks are drawn as lines only up to a radius of 50 cm so as not to obscure the TRT hits. The small box selects a part of a pion track from the K_s^0 decay and of an electron track from a J/ψ decay (see Fig. 2).

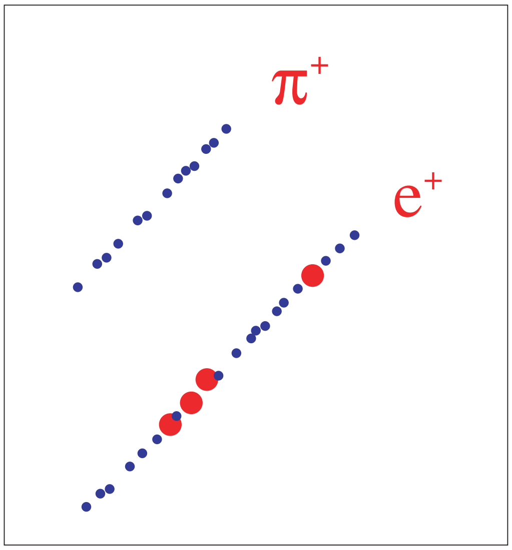

Fig. 2. Expanded view of the portion of the tracks within the box in Fig. 1. The electron track contains many more high-threshold hits (larger points) than the pion track. Electron identification via transition radiation is based on this difference (see text).

Particle identification using only the information from the low-threshold discriminator has also been shown to be possible [5–7]. A time-over-threshold technique for straw tubes, similar to the one discussed in this paper, has been studied in [5], whereas the discriminator leading-edge information corrected as a function of track distance from the wire was used in [6].

In this paper, a time-over-threshold method which includes corrections for the track position inside the straw is discussed. The time-over-threshold is defined as the width of the low-threshold discriminator signal. This signal width is larger for signals with larger amplitudes. However, this width also depends on the track position inside the straw, as illustrated in Fig. 3. For a track crossing the straw near the anode wire, the signal width is obviously larger than for the case when the track crosses the straw near the cathode. In order to extract information about the energy loss of a particle, it is important to correct for this dependence. This results in a significant improvement of the TRT particle identification capability with respect to the method without track-position correction used in [5], as shown in Section 2.2.2. The time-over-threshold method with track-position correction improves particle identification in the TRT at low particle momenta. The average energy losses expected for electrons, pions and kaons as they travel through the TRT Xe-based gas mixture, are shown as a function of momentum in Fig. 4. These curves suggest that improved e/π separation may be possible for momenta below than 10 GeV and that K/π separation may be possible over the momentum range relevant for B-physics at the LHC (see Section 3).

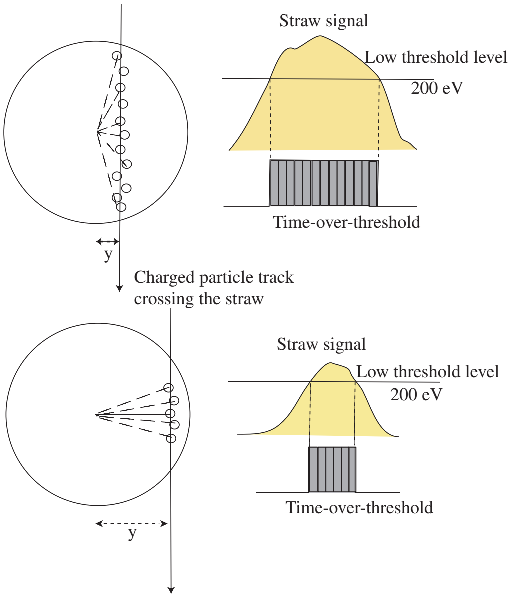

Fig. 3. Dependence of the time-over-threshold on the track distance, y, from the wire. The straw signal is shown before and after the low-threshold (200 eV) discrimination.

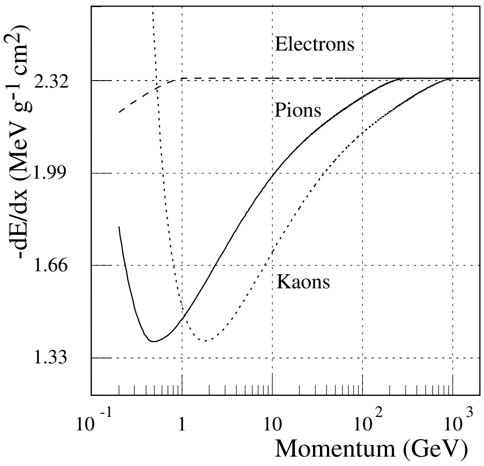

Fig. 4. Bethe-Bloch curves for various particles in the ATLAS TRT gas mixture. For momenta less than 20 GeV, good particle identification based on an accurate measurement of the energy loss is possible.

2 Electron-pion separation

2.1 Experimental set-up

The performance of the time-over-threshold method for electron-pion separation was evaluated in the H8 beam line at the CERN SPS. Pion and electron beams of different energies were used (20, 10 and 5 GeV).

The experimental set-up is shown in Fig. 5. It included a small straw prototype used for precise ionisation loss and transition-radiation measurements ('ADC straws'), and a single straw used for time-over-threshold measurements ('ToT straw'). Other equipment consisted of two standard multiwire beam chambers (BC1 and BC2) for a first coarse track reconstruction, of two silicon detectors (Si1 and Si2) with an intrinsic accuracy of about 10 μm, which provided a very precise reconstruction of the beam track position in the TRT straws, and of two small scintillators (s1 and s2) used in coincidence as the trigger. Two Cerenkov detectors and a lead-glass calorimeter were also read out and used for particle identification.

The straw prototype, placed between the two silicon detectors, had 10 layers of straw drift-tubes, optionally interleaved with radiator (the presence and type of the radiator was run-dependent), and was read out with conventional ADCs. The information from these drift-tubes was used to tune the Monte-Carlo model and to study the transition-radiation performance of different radiators inserted between them. The single straw used for the time-over-threshold method was placed behind the second silicon detector, and was rotated by 21° from the perpendicular to the beam. A 12 cm thick fibre radiator was positioned in front of this straw, in order to simulate a straw at $|\eta| = 0.3$ in the ATLAS barrel TRT (see Section 2.3.2). This single straw was equipped with an amplifier-shaper-discriminator (ASDBLR), with low-level (200 eV) and high-level (5 keV) discriminator thresholds. For this study, the discriminated signal was fed into a multi-hit TDC, with a 1 ns resolution, that provided leading and trailing edge information both for low and high-threshold signals. In the final version of the ATLAS TRT front-end electronics, this information is extracted using an amplifier-shaper-discriminator (ASDBLR) and a time digitiser (DTMROC). In the ASDBLR the signal is amplified, shaped and two-fold discriminated. In the DTMROC the low-threshold discriminated pulse is digitised in 3.125 ns time bins. This bin size has been chosen as an acceptable compromise between the measurement accuracy and data bandwidth requirements [8]. From the DTMROC readout the time of the leading and trailing edge of the low-threshold discriminator signal and the possible presence of the high-threshold discrimination level are determined.

Standard TRT 4 mm diameter Kapton straws with a 30 μm diameter gold-plated tungsten wire were used. The straws were 10 cm in length. The ionisation gas mixture was 69.5%Xe + 22%CF_4 + 8.5%CO_2, very close to the one which will be used for the ATLAS TRT (70%Xe + 20%CF_4 + 10%CO_2). This gas mixture provides good absorption for photons in the X-ray region, a short total drift time of about 40 ns and good operational stability with respect to discharges. The gain was set to $2.5{\cdot}10^4$ and stabilised through a high-voltage feedback loop with an accuracy of better than 1%, as nominally required for operation in ATLAS .

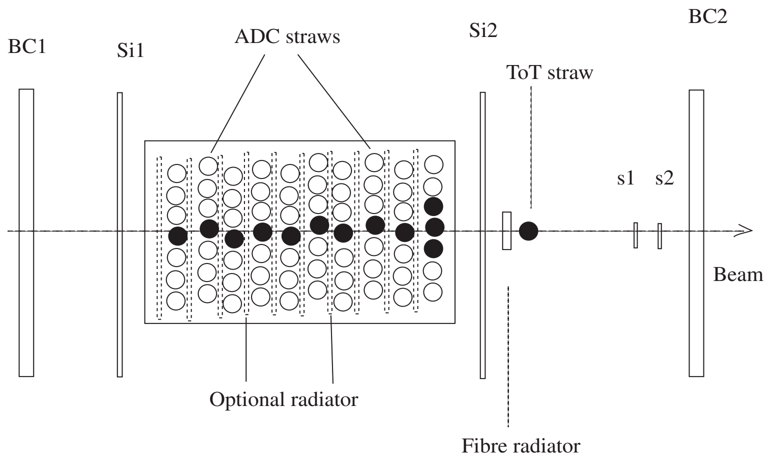

Fig. 5. Schematic view of the experimental set-up (not to scale). MWPC's (BC1 and BC2) and silicon detectors (Si1 and Si2) were used for tracking, two scintillators (s1 and s2) were used in coincidence for triggering. Straws for radiator studies (ADC straws), the single straw for the time-over-threshold studies (ToT straw) and the radiator locations are also indicated. The straws that were read out are represented as black circles.

2.2 Data analysis

2.2.1 Time-over-threshold studies with a single straw

The results of the data analysis for the 'ToT straw' in the experimental set-up with all radiators in place (see Fig. 5) are discussed in this section. For this configuration, the amount of transition radiation generated by the 5, 10 and 20 GeV electrons corresponded to a probability of about 26% per straw for high-threshold hits, with energy above 5 keV, close to that expected in the ATLAS barrel TRT (see Section 2.3.2).

With incident pions, the high-threshold hit probability was about 6%, mostly due to large energy depositions caused by δ-rays, again close to that expected in the ATLAS barrel TRT.

Since there was no magnetic field, the track reconstruction was performed using a simple linear fit. A coarse track was reconstructed using hits from BC1 and BC2, and the track fit was then refined using the very accurate information from the silicon detectors. The straw was aligned by minimising the residual between the predicted position of the track within the straw and the position calculated using the drift-time information. A spatial resolution ranging between 125 μm at 20 GeV and 155 μm at 5 GeV was achieved. The degradation at lower energy is due to multiple scattering in the material of the set-up.

The time-over-threshold method was evaluated in a way compatible with the ATLAS TRT electronics read out, by emulating the 3.125 ns DTMROC binning using the data obtained from the 1 ns TDC.

The uncorrected time-over-threshold data obtained in this way for the ToT straw and for 5 GeV pions (solid line) and electrons (dotted line) are shown in Fig. 6 and Fig. 7. In Fig. 6, only hits without high-threshold discriminator level are included, since they provide a sample of hits used subsequently to build up a discriminating variable totally independent of the standard transition-radiation cluster-counting technique. In Fig. 7, all the hits are considered, and the difference between pions and electrons is, as expected, enhanced with respect to Fig. 6. The larger values in the time-over-threshold distributions of Fig. 7 are dominated by transition radiation for electrons and by δ-rays for pions.

The correlation between the uncorrected time-over-threshold and the distance of closest approach to the wire for 5 GeV pion data is shown in Fig. 8 for the sample without high-threshold hits. For a track crossing the straw close to the anode wire, the electron clusters are produced along a length equal to the straw diameter, as sketched in Fig. 3 . In order to parameterise this dependence, the straw was divided into 200 μm bins and the time-over-threshold was evaluated for each bin. The parameterisation used a cubic polynomial.

The time-over-threshold residual, Δ_{ToT}, is then calculated as a function of y by subtracting the parameterised pion time-over-threshold ($ToT_{\pi fit}(y)$) from the measured time-over-threshold ($ToT_{meas.}(y)$):

$$\Delta_{ToT} = ToT_{meas.}(y) - ToT_{\pi fit}(y).$$

This residual does not depend on the distance of closest approach (and therefore on the track length), as can be seen in Fig. 9. The values for pions are centred at zero, as expected, whereas those for electrons are shifted upwards on average by about 1.5 ns. The corrected Δ_{ToT} distributions for 5 GeV pions (solid line) and electrons (dotted line) are shown in Fig. 10 for straws without high-threshold hits.

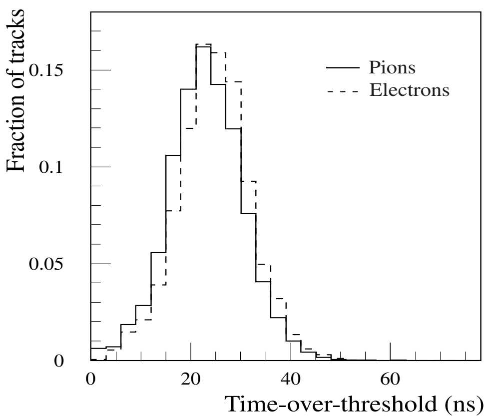

Fig. 6. Uncorrected time-over-threshold distributions for 5 GeV pions and electrons for hits without high-threshold discriminator level.

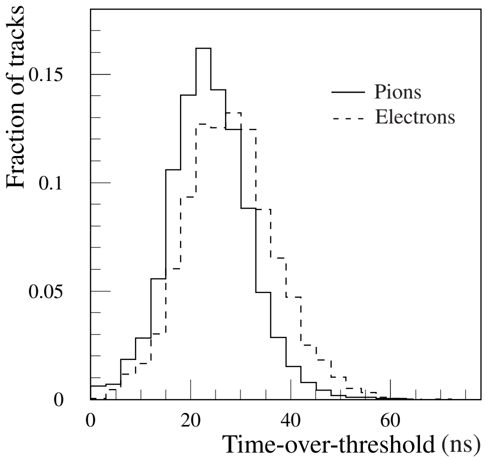

Fig. 7. Uncorrected time-over-threshold distributions for 5 GeV pions and electrons for all hits.

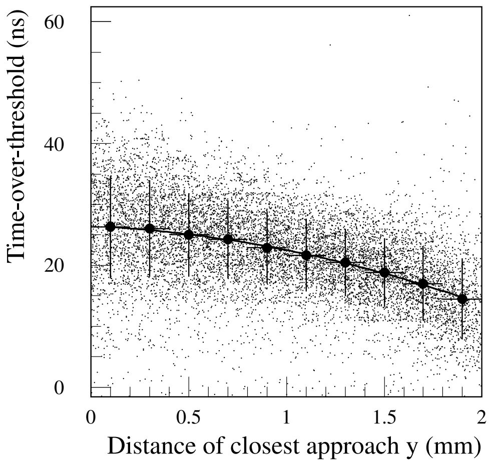

Fig. 8. Parameterisation of the dependence of time-over-threshold upon the distance of closest approach to the anode wire (y) for 5 GeV pions. The points represent the mean value for each y bin of width 200 μm, and the error bars represent the r.m.s. of the time-over-threshold distribution in each y bin.

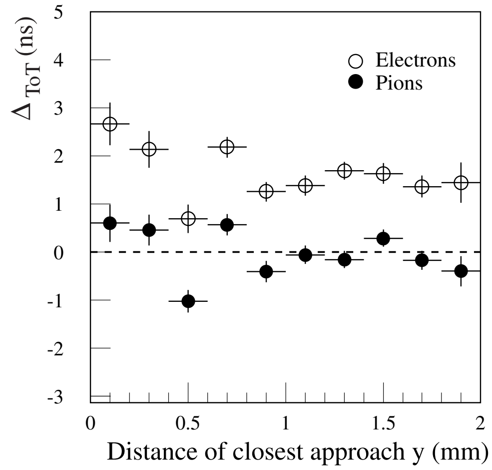

Fig. 9. Correlation between the corrected time-over-threshold residuals (Δ_{ToT}) and the distance of closest approach for 5 GeV pions and electrons. The points represent the mean value for each y bin, and the error bars represent the statistical uncertainty on these mean values.

2.2.2 Time-over-threshold studies with pseudo-tracks

The energy loss measurements described above in detail for a single straw provide a powerful method for particle identification in gaseous detectors with

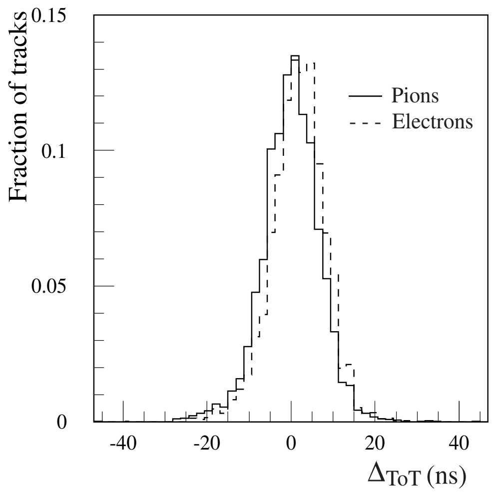

Fig. 10. Corrected time-over-threshold residuals, Δ_{ToT}, for a single straw without high-threshold hits and for samples of 5 GeV pions and electrons (see text).

many measurements available along the same track.

In the test-beam, there was just one straw, providing a single time-over-threshold measurement per track. In the ATLAS TRT, there will be on average 35 straws crossed per track and a large fraction of those will give a hit (i.e. will yield a measured drift time within a two-standard-deviation window from the reconstructed position of the track). The hit efficiency depends partially on η and largely on luminosity [9]. For the study shown in this section, which will be compared to ATLAS prediction for single tracks at $\eta = 0.3$ (see Section 2.3.2), an hit efficiency of $\sim 90\%$ is assumed. To simulate crudely the situation expected in the ATLAS experiment, pseudo-tracks were therefore created by randomly combining 32 hits (with a gaussian spread of three hits) from different test-beam events. This analysis was performed with 30000 pseudo-tracks for each beam energy and particle type.

A discriminating variable, $< \Delta_{ToT} >$, is formed by averaging the time-over-threshold residuals from n straws along the pseudo-track:

$$< \Delta_{ToT} > = \frac{\sum_i \Delta^i_{ToT}}{n} \text{ for } i = 1,...,n$$

Two $< \Delta_{ToT} >$ variables were studied: one used all hits available on the track; the other used only the hits without high-threshold discriminator level. These $< \Delta_{ToT} >$ distributions for pseudo-tracks are shown in Fig. 11 (no high-threshold hits) and Fig. 12 (all hits). The distributions of the number of high-threshold hits along the reconstructed pseudo-tracks are shown in Fig. 13 for 5 GeV pions and electrons. These distributions are the standard ones used for electron-pion separation using transition radiation.

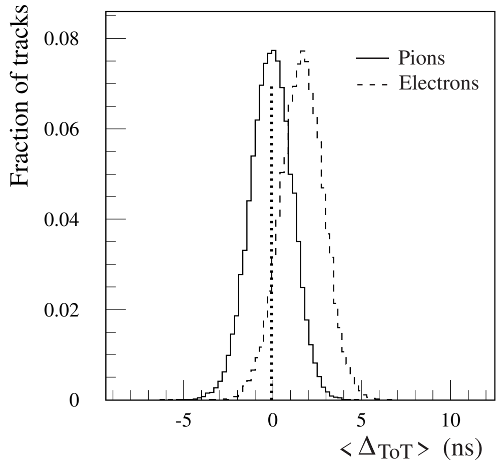

Fig. 11. $< \Delta_{ToT} >$ (no high-threshold hits) for 5 GeV pseudo-tracks. The vertical line represents the $< \Delta_{ToT} >$ value for a 90% electron efficiency.

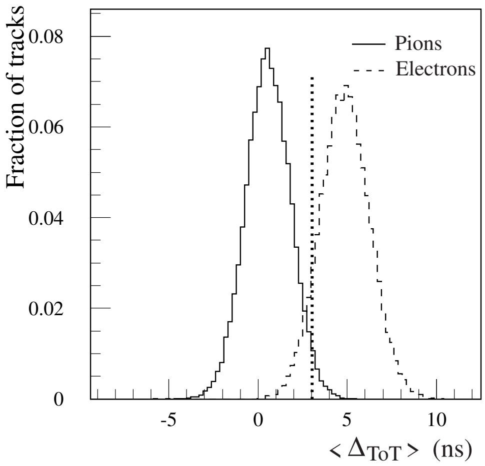

Fig. 12. $< \Delta_{ToT} >$ (all hits) for 5 GeV pseudo-tracks. The vertical line represents the $< \Delta_{ToT} >$ value for a 90% electron efficiency.

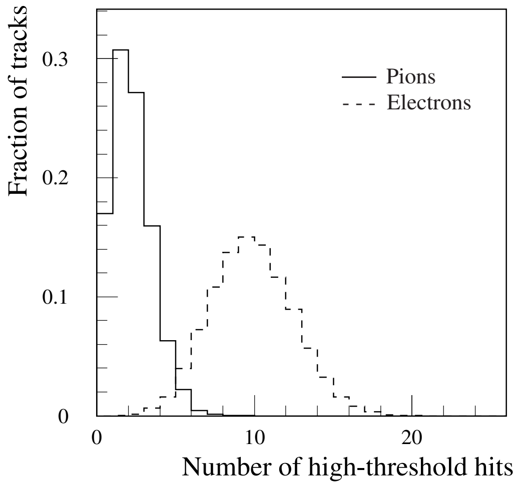

Fig. 13. Number of high-threshold hits for 5 GeV pseudo-tracks.

2.2.3 Performance obtained for electron-pion separation

As illustrated in Fig. 12, an electron of 5 GeV can be identified with 90% efficiency, using the time-over-threshold technique described above, by requiring that $< \Delta_{ToT} >$ is above 3 ns. The fraction of pions passing this cut represents the pion misidentification probability. This pion misidentification probability is shown in Fig. 14 as a function of the electron efficiency for the two $< \Delta_{ToT} >$ variables, namely using all hits (large open circles) and using only hits without high-threshold discriminator level (large black circles). When $< \Delta_{ToT} >$ is used as the only discriminating variable, much better electron-pion separation is obtained of course if all the hits on the track are used. In particular, a pion misidentification probability as low as 2.6% can be achieved for a 90% electron efficiency at 5 GeV. To illustrate the importance of the correction for the track position inside the straw (discussed in Section 2.2.1), the results without this correction (small circles) are also shown in Fig. 14. In the case where all hits are used, the improvement obtained by using this correction is about a factor 2.5 for an electron efficiency of 90%.

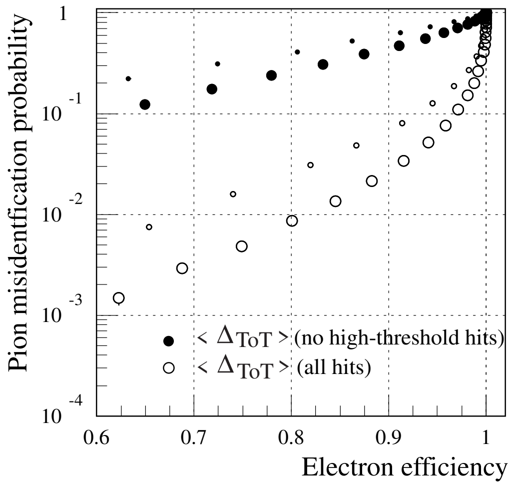

Fig. 14. Pion misidentification probability versus electron efficiency, as obtained using $< \Delta_{ToT} >$ at 5 GeV for pseudo-tracks constructed from the test-beam data. The open circles are calculated using all the hits along the pseudo-track, whereas the black circles are calculated using only hits without high-threshold discriminator level. The large (resp. small) circles correspond to $< \Delta_{ToT} >$ corrected (resp. uncorrected) for the track position inside the straw.

In order to obtain the best possible electron-pion separation, the time-over-threshold has to be combined with the cluster-counting technique, that uses the number of high-threshold hits along the track. The correlation between $< \Delta_{ToT} >$ and the number of high-threshold hits is shown in Fig. 15 ($< \Delta_{ToT} >$ without high-threshold hits) and Fig. 16 ($< \Delta_{ToT} >$ with all hits) for 5 GeV electrons and pions. While there is now one more degree of freedom for optimising electron identification, the two discriminating variables are correlated. The correlation is clearly stronger, as expected, when Δ_{ToT} is averaged over all the hits on the pseudo-track.

A likelihood analysis has been performed to combine the two variables in an optimal way for three different test-beam energies of 5, 10 and 20 GeV. In Table 1, the pion misidentification probability at 90% electron efficiency for various time-over-threshold methods, for the cluster-counting technique and for the combined method is tabulated as a function of energy. The comparison between the electron-pion separation achieved at 5 GeV with the cluster-counting technique and the combined method is shown in Fig. 17, which can also be compared to Fig. 14, where only the time-over-threshold information

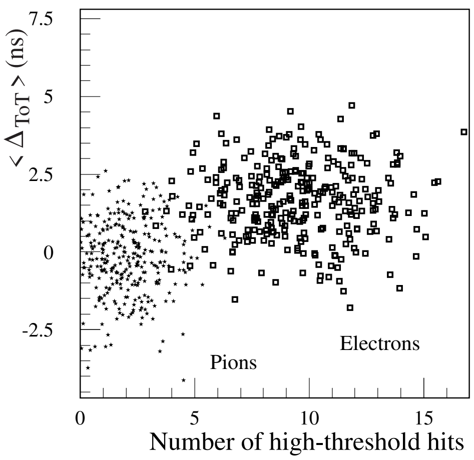

Fig. 15. Distribution of $< \Delta_{ToT} >$ (no high-threshold hits) versus number of high-threshold hits for 5 GeV pseudo-tracks. Electrons are plotted as open squares and pions as black stars.

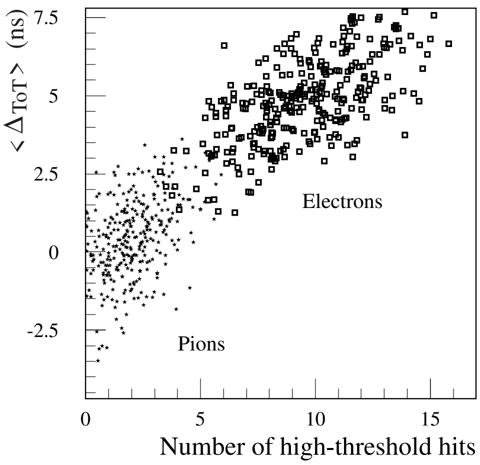

Fig. 16. Distribution of $< \Delta_{ToT} >$ (all hits) versus number of high-threshold hits for 5 GeV pseudo-tracks. Electrons are plotted as open squares and pions as black stars.

is used. Table 1 clearly demonstrates that the transition-radiation information provides a rejection which is a factor 3.5 to 6 higher than that obtained with time-over-threshold alone. Nevertheless, the pion misidentification probability at 5 GeV and at 90% electron efficiency improves by a factor of two for the combined method with respect to the standard transition-radiation cluster-counting technique alone.

Table 1
For a 90% electron efficiency and for pseudo-tracks constructed from test-beam data at three different energies, pion misidentification probability obtained using different techniques (see text).

Method	$E_b = 5\,\mathrm{GeV}$	$E_b = 10\,\mathrm{GeV}$	$E_b = 20\,\mathrm{GeV}$
Time-over-threshold (no high-threshold hits)	0.46 ± 0.01	0.58 ± 0.01	0.73 ± 0.01
Time-over-threshold (all hits, no y correction)	0.067 ± 0.002	0.10 ± 0.01	0.17 ± 0.01
Time-over-threshold (all hits)	0.026 ± 0.001	0.041 ± 0.001	0.10 ± 0.002
Number of high-threshold hits	0.0072 ± 0.0003	0.012 ± 0.001	0.017 ± 0.001
Combined method	0.0037 ± 0.0002	0.008 ± 0.001	0.016 ± 0.001

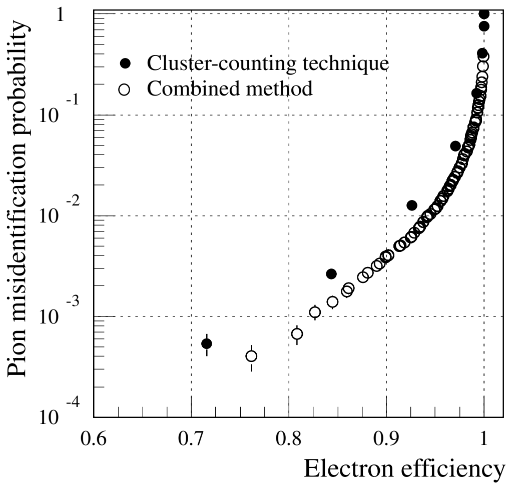

Fig. 17. Pion misidentification probability versus electron efficiency at 5 GeV for pseudo-tracks constructed from test-beam data. The results are shown for the standard cluster-counting technique and for the combined method using also the time-over-threshold information (see text and Table 1).

2.3 Monte Carlo simulation and comparison to test-beam data

2.3.1 Monte Carlo model

A Monte Carlo model, based on GEANT 3.21 [10], has been developed to simulate the straws and the other detectors in the beam line [11]. It includes detailed models to describe the energy deposition in the straws, transition-radiation creation and absorption and the response of the front-end electronics [12]. The energy loss for each charged particle crossing the ionisation gas is calculated using the Photo-Absorption Ionisation (PAI) model [13]. This ionisation is deposited over a small (typically $\sim$ 50 per cm for minimum-ionising particles, while $\sim$ 70 per cm for particles at the Fermi plateau) number of primary ionisation centres along the path length. In addition, for a charged particle with a Lorentz factor above 1000, transition-radiation photons are generated in the radiator material, according to the formulae given in [14,15]. This photon spectrum is transported along the particle track, partially absorbed in the radiator itself, in the straw walls, and in the gas mixture inside the straws. Transition-radiation photons deposit point-like ionisation clusters in the same straws as those crossed by the parent particle. All the primary clusters are then allowed to drift towards the anode, as shown in Fig. 3, and the signal amplitudes and arrival times on the wire are summed over all primary clusters for all charged particles crossing each straw. Space-charge effects, that cause a reduction in the gain for large energy depositions are also simulated. This summed signal is then folded with a model of the electronics signal shape as shown in Fig. 18. The resulting signal is finally discriminated and digitised in 3.125 ns bins.

In order to compare the PAI model with experimental data in detail for the

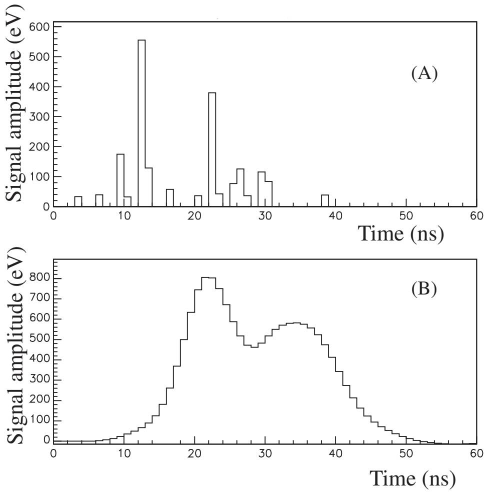

Fig. 18. Monte Carlo simulation of the straw signal. A) The ionisation clusters drift towards the anode and the signal amplitudes and arrival times are recorded. (B) The straw output signal is then convoluted with a model of the response of the front-end electronics.

ionisation losses of pions and electrons, the pulse-height information from the straw prototype (for the configuration without radiators) placed between the two silicon detectors was used. The comparison between the Monte Carlo and experimental differential energy spectra is shown in Fig. 19 and 20, respectively for 5 GeV pions and electrons. The most probable energies are 1.1 keV for pions and 1.3 keV for electrons. The integral energy deposition spectra for 5 GeV pions and electrons and for data and Monte Carlo are shown in Fig. 21. The integral spectra are obtained from the differential spectra above the low threshold of 0.2 keV, chosen for the operation of the ATLAS TRT front-end electronics.

The good agreement observed between the Monte Carlo and the experimental data for the differential and integral spectra above 0.2 keV is an essential ingredient in the work required to obtain reliable predictions for the electron-pion separation to be expected in ATLAS using the methods described above. For both the Monte Carlo and the data time-over-threshold analysis, the same software chain has been used. The pion misidentification probability at 90% electron efficiency is shown in Fig. 22 as a function of energy for the test-beam data at 5, 10 and 20 GeV and for the Monte Carlo simulation. The results are shown for pseudo-tracks and for the various methods described above. Additional Monte Carlo simulation results at lower energies (1 and 2 GeV) are also shown in Fig. 22. The four sets of points (data) and lines (Monte Carlo) represent (in order of decreasing pion misidentification probability) the time-

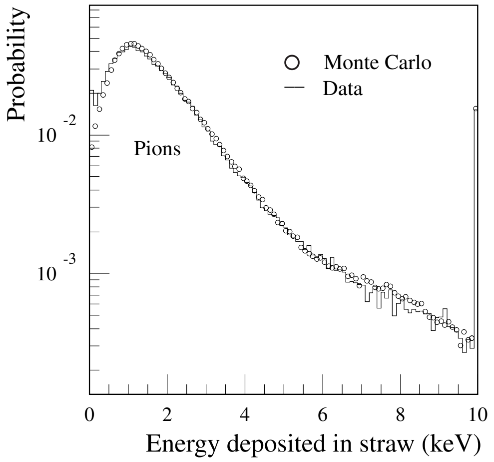

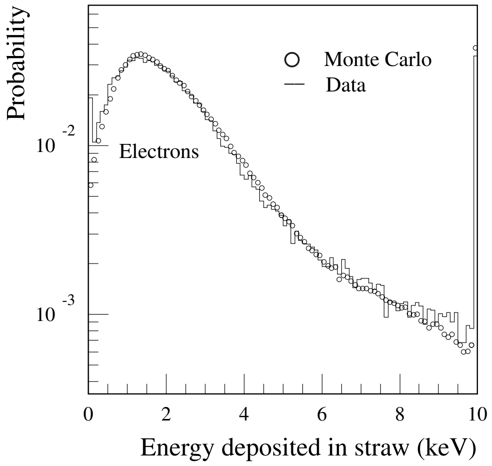

Fig. 19. For a single straw without radiator and for 5 GeV pions, differential energy spectra from test-beam data (histograms) and Monte Carlo simulation (open circles).

Fig. 20. For a single straw without radiator and for 5 GeV electrons, differential energy spectra from test-beam data (histograms) and Monte Carlo simulation (open circles).

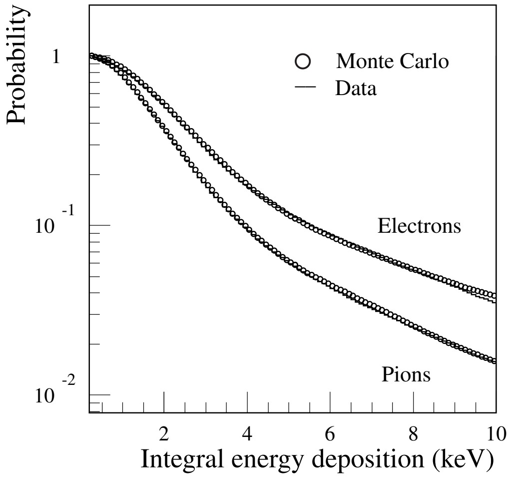

Fig. 21. Integral energy deposition spectra (integrated above 0.2 keV) for 5 GeV pions and electrons, as measured in the test-beam and predicted by Monte Carlo simulations for a single straw without radiator.

over-threshold method alone (without using high-threshold hits and using all hits), the cluster-counting technique alone and the overall combined method. In the lower-energy region (1-2 GeV), where transition radiation production is not yet saturated, the time-over-threshold method is expected to improve the overall electron-identification performance by up to one order of magnitude.

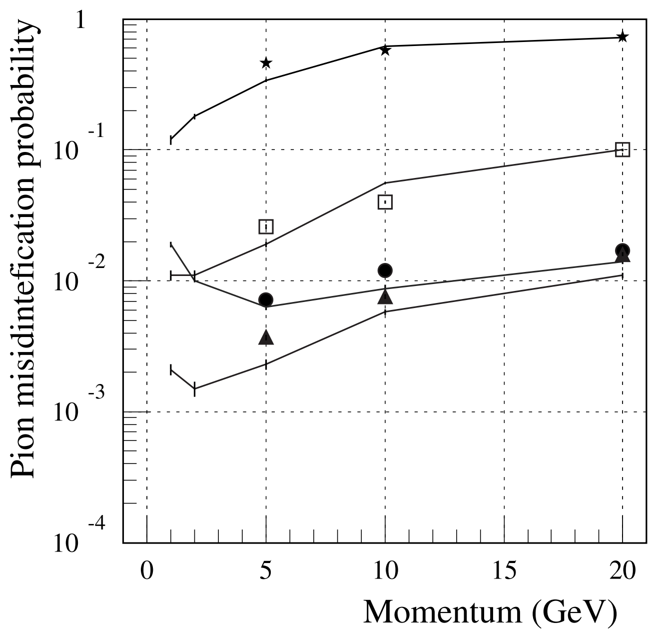

Fig. 22. Pion misidentification probability as a function of momentum at 90% electron efficiency for pseudo-tracks in the test-beam setup. The performance is shown for $< \Delta_{ToT} >$, without using high-threshold hits (stars), for $< \Delta_{ToT} >$ using all hits (squares), for the transition-radiation cluster-counting technique (circles) and for the overall combined method (triangles). The test-beam data results at 5, 10 and 20 GeV are shown as points, while the Monte Carlo simulation results are shown as lines from 1 GeV to 20 GeV. The errors shown are statistical (above 5 GeV the errors are often smaller than the symbols).

2.3.2 Expected performance for e/π separation in the ATLAS TRT

The ATLAS Inner Detector is described in detail in [1]. It combines high-resolution silicon detectors (using both pixel and micro-strip technologies) at the inner radii with the 'continuous' tracking elements of the TRT at the outer radii, all contained in a 2T solenoidal magnetic field.

The electron-pion separation was studied in more detail for the ATLAS TRT by using the full simulation (based on GEANT 3.21) of single particles without pile-up and with the overall straw response tuned to test-beam data. Tracks were generated in the barrel TRT, in a narrow region around $\eta = 0.3$ ($0.29 < \eta < 0.31$) and at different momenta. This η region corresponds approximately to the incidence angle of 21° of the beam tracks with respect to the straw axis in the test-beam setup, and gives on average 32 hits per track (see Section 2.2.2).

These detailed studies are necessary to validate the time-over-threshold predictions reported in Section 2.3.1, due to the somewhat different radiator geometry in the test-beam setup and since pseudo-tracks do not take into account possible correlations between successive straws on a track. Such correlations are expected to be energy-dependent to some extent and are due, in particular, to hadronic interactions, electromagnetic showers, high energy δ-rays and transition radiation. The reconstruction of the tracks was performed using a standard ATLAS pattern recognition code, which starts by associating hits in the TRT and then projects the track candidates back to the silicon hits [16].

The resulting pion misidentification probability is shown in Fig. 23 as a function of p_{T}, for a 90% electron efficiency and for the different methods discussed above. For a transverse momentum of 5 GeV, the time-over-threshold method

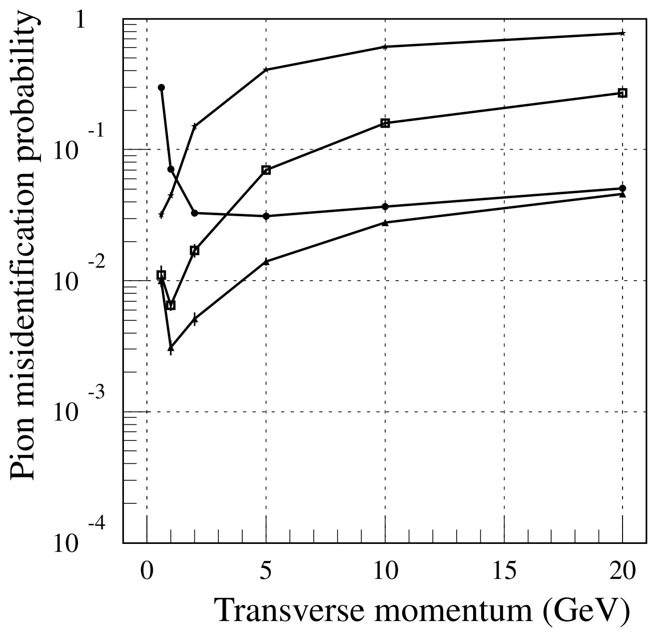

Fig. 23. Pion misidentification probability as a function of transverse momentum at 90% electron efficiency for simulated single tracks at $\eta = 0.3$ in the ATLAS Inner Detector without pile-up. The performance is shown for $< \Delta_{ToT} >$ without using high-threshold hits (stars), for $< \Delta_{ToT} >$ using all hits (squares), for the transition-radiation cluster-counting technique (circles), and for the overall combined method (triangles).

improves the overall TRT performance by a factor of two, while at even lower energies of 1-2 GeV the improvement is expected to be as large as one order of magnitude, in agreement with the test-beam data pseudo-track predictions discussed in Section 2.3.1.

2.3.3 Comparison between pseudo-tracks and the full ATLAS Monte Carlo

The performance predicted for the electron-pion separation with the full ATLAS simulation (see Fig. 23) is consistent with the studies done with pseudo-tracks obtained from test-beam data (see Fig. 22) for the time-over-threshold method without using high-threshold hits. However, the predicted performance of the time-over-threshold method with all hits, of the cluster-counting technique and of the combined electron-pion separation are significantly worse in the case of the ATLAS barrel TRT Monte Carlo.

In order to separate out the effect due to transition radiation from other effects, such as possible correlations between successive straws along a track (neglected obviously in the pseudo-track analysis described in Section 2.2), the radiator model used for the full ATLAS barrel TRT Monte Carlo was tuned to roughly reproduce the test-beam transition-radiation yields. As a result of this tuning, the radiator yield in the ATLAS barrel TRT Monte Carlo had to be increased by 20% to account for the differences between the radiator used in the test-beam and the radiator planned to be used for the barrel TRT. Tracks were then generated in the barrel TRT and compared to test-beam Monte Carlo pseudo-tracks, that have been shown in Section 2.3.1 to reproduce reliably the test-beam data. The resulting pion misidentification probabilities at 90% electron efficiency are tabulated in Table 2, for the transition-radiation cluster-counting technique, the time-over-threshold method without high-threshold hits and the time-over-threshold method with all hits. The results are shown as a function of momentum for fully simulated tracks and for test-beam pseudo-tracks.

The results now show a good agreement between the predictions from barrel TRT tracks with tuned radiator performance and from test-beam pseudo-tracks, in the case of the standard transition-radiation cluster-counting technique. The discrepancies observed between test-beam pseudo-tracks and barrel TRT tracks, in the case of the time-over-threshold methods, are significant (up to $\sim 50\%$ in terms of pion misidentification probability) and are most likely due to the correlation effects mentioned above.

Table 2
For a 90% electron efficiency, for different techniques and for different momenta, pion-misidentification probability as obtained from barrel TRT tracks and test-beam pseudo-tracks. The barrel TRT tracks were simulated at $\eta = 0.3$, corresponding to an incident angle close to the test-beam one. The performance obtained with the standard transition-radiation cluster-counting technique are tabulated in the first block, while the performance obtained with the time-over-threshold method without high-threshold hits (resp. with all hits) are tabulated in the second (resp. third) block.

Monte Carlo tracks type	p = 5 GeV	p = 10 GeV	p = 20 GeV
TR technique			
Barrel TRT tracks	0.007 ± 0.001	0.008 ± 0.001	0.012 ± 0.001
Test-beam pseudo-tracks	0.006 ± 0.001	0.009 ± 0.001	0.014 ± 0.001
ToT method (no HT hits)			
Barrel TRT tracks	0.41 ± 0.01	0.61 ± 0.01	0.77 ± 0.01
Test-beam pseudo-tracks	0.34 ± 0.01	0.62 ± 0.01	0.72 ± 0.01
ToT method (all hits)			
Barrel TRT tracks	0.031 ± 0.001	0.075 ± 0.001	0.14 ± 0.01
Test-beam pseudo-tracks	0.019 ± 0.001	0.056 ± 0.001	0.10 ± 0.01

3 Expected performance for K/π separation in the ATLAS TRT

Hadron identification is obviously important for many aspects of B-physics studies, in the ATLAS experiment [17]. Earlier Monte Carlo studies of K/π separation using signal shape information from the ATLAS TRT are reported in [6]. In that work, only the expected shift in the time of the leading edge as a function of particle mass was used, and a maximum K/π separation of 0.9 standard deviation was predicted at 5 GeV momentum.

In this paper, the time-over-threshold method is used, assuming that the TRT readout will provide this information at low luminosity while preserving the output bandwidth requirements. The analysis of the time-over-threshold follows the same procedure as described above and, obviously, all hits are used in this case. The expected $< \Delta_{ToT} >$ distributions for reconstructed tracks in the ATLAS barrel TRT at $|\eta| = 0.3$ are shown in Fig. 24 for 5 GeV pions and kaons. The expected K/π separation as a function of transverse momentum is shown in Fig. 25 in units of standard deviation. Without including any pile-up effects, the K/π separation is predicted to be above one standard deviation for transverse momenta between 2 and 5 GeV, averaged over the full rapidity coverage (solid line), and above one standard deviation over a broader p_{T}-range between 2 and 15 GeV at $|\eta| = 0.3$ (dotted line).

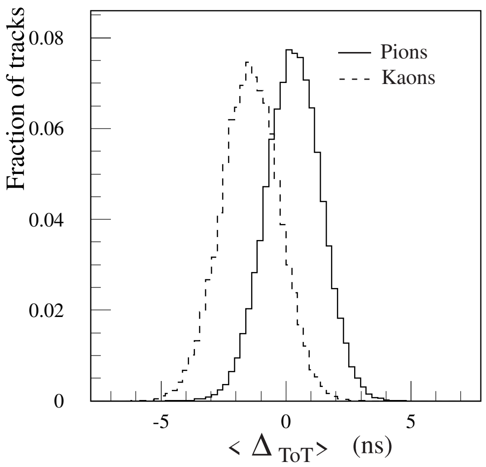

Fig. 24. $< \Delta_{ToT} >$ (all hits) for reconstructed tracks in the ATLAS barrel TRT at $|\eta| = 0.3$ for 5 GeV pions (solid line) and kaons (dashed line).

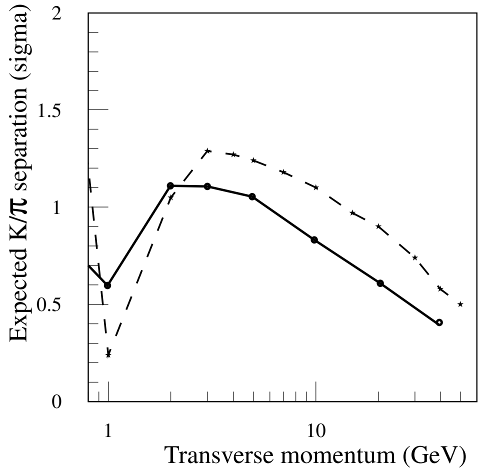

Fig. 25. Expected K/π separation in the ATLAS TRT as a function of transverse momentum (no pile-up effects included). The separation is shown as an average over the full rapidity coverage (solid line) and at $|\eta| = 0.3$ (dotted line).

As an example of the importance of having some K/π separation (and, more generally, hadron identification) in ATLAS, the results of this study have been applied to the $B_d^0 \to \pi^+\pi^-$ decay, which is useful for extracting information about the angle α of the unitarity triangle used for CP-violation studies. The two-pion final state of the B_d^0 decay is plagued by various sources of background, mostly three or two-body decays involving also kaons and protons. The predicted $\pi^+\pi^-$ invariant mass spectrum for the ATLAS experiment, after three years of low-luminosity data-taking at the LHC is shown in Fig. 26, using recent values of the B_d^0 branching ratios (as quoted in [18]), and for a scenario without hadron identification in the ATLAS TRT. The signal is represented by the dark shaded area, while the various backgrounds (most of which lie just on top of the signal) are represented as lighter shaded regions [18]. As an illustration, the corresponding predicted $\pi^+\pi^-$ invariant mass spectrum when dE/dx information (via the time-over-threshold measurements in the TRT) is used is shown in Fig. 27, for a 50% efficiency for the $B_d^0 \to \pi^+\pi^-$ signal. The fraction of the signal in a window around the B_d^0 mass improves from a value of 15% to a value of 21%. The accuracy of the measurement of the $B_d^0 \to \pi^+\pi^-$ asymmetry, which makes use of dE/dx information together with other information in an event-by-event maximum likelihood, is improved by about 35% with respect to the scenario without hadron identification in the ATLAS Inner Detector.

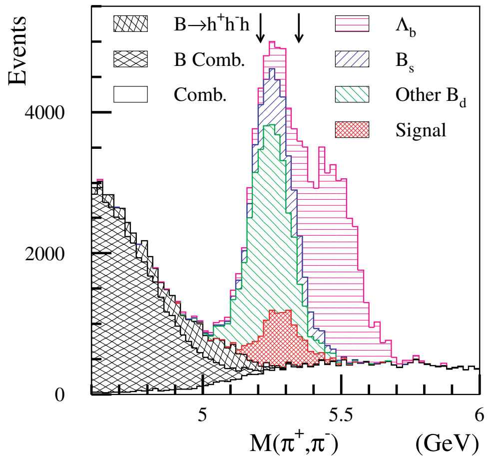

Fig. 26. $\pi^+\pi^-$ mass spectrum in the ATLAS experiment for B_d^0 signal and various backgrounds and for the scenario without kaon-pion separation in the ATLAS TRT.

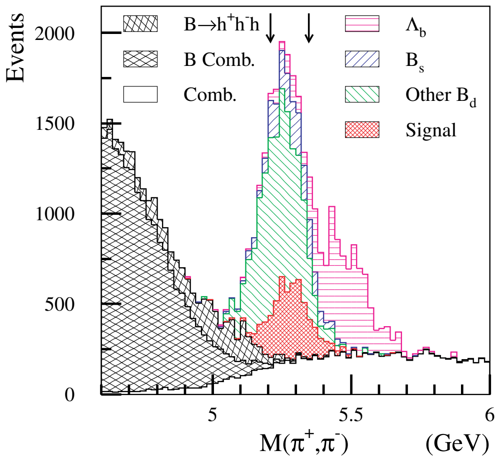

Fig. 27. $\pi^+\pi^-$ mass spectrum in the ATLAS experiment for B_d^0 signal and various backgrounds and for the scenario with a kaon-pion separation in the ATLAS TRT as predicted by the study presented in this paper (see text).

4 Conclusions

Using test-beam data taken at the CERN SPS with 5, 10 and 20 GeV pion and electron beams, time-over-threshold measurements, using the front-end electronics planned for the operation of the ATLAS TRT at the LHC, have demonstrated that significant particle identification can be achieved over an interesting range of particle types and energies.

Electron-pion separation at energies below 10 GeV can be significantly enhanced by combining the standard transition-radiation cluster-counting technique with the time-over-threshold information. In particular, pion misidentification probabilities below $4 \cdot 10^{-3}$ can be reached at 90% electron efficiency for energies between 1 and 5 GeV. This measured test-beam performance leads to expected pion misidentification probability of about 10^{-2} at 90% electron efficiency over the same energy range in the ATLAS barrel TRT.

Detailed Monte Carlo studies are shown to reliably reproduce the test-beam results. The extrapolation to K/π separation in the field of B-physics at the LHC leads to the conclusion that the ATLAS B-physics potential would be significantly improved through the use of time-over-threshold measurements in the ATLAS TRT.

5 Acknowledgements

Work was partially supported by grant nr. 620/E-77/SPUB/CERN/P-03/DZ 2/9 of the Polish Committee for Scientific Research (KBN).

References

[1] ATLAS Inner Detector Technical Design Report, CERN/LHCC/97-17, ATLAS TDR 5 (1997).

[2] J. T. Shank et al., Nucl. Instr. and Meth. in Phys. Res., A310 (1991) 133.

[3] T. Akesson et al., Nucl. Instr. and Meth. in Phys. Res., A372 (1996) 70.

[4] T. Akesson et al., Nucl. Instr. and Meth. in Phys. Res., A412 (1998) 200.

[5] V. Bashkirov and B. Dolgoshein, ATLAS INDET-No-090 (1994).

[6] ATLAS Detector and Physics Performance Technical Design Report, CERN/LHCC/99-14,15, ATLAS TDR 14 (1999), p. 74-76 and ATLAS TDR 15 (1999) p. 577-582.

[7] V. Bashkirov, Nucl. Instr. and Meth. in Phys. Res., A433 (1999) 560.

[8] T. Akesson et al., Straw-Tube Drift-Time Properties and Electronics Parameters for the ATLAS TRT Detector, to be published in NIM.

[9] ATLAS Inner Detector Technical Design Report, CERN/LHCC/97-16, ATLAS TDR 4 (1997), p. 95-96.

[10] CN division Application Software group, GEANT detector description and simulation tool, CERN Program Library Long Writeup W5013, 1993

[11] A. Artamonov et al, "DICE-95", internal note ATLAS-SOFT/95-14, CERN (1995).

[12] ATLAS Inner Detector Technical Design Report, CERN/LHCC/97-16, ATLAS TDR 4 (1997), p. 90-91.

[13] V.M. Grishin, V.K. Ermilova, S.K. Kotelnikov, Nucl. Instr. and Meth. in Phys. Res., A307 (1991) 273.

[14] M. Cherry, G. Hartmann, D.Muller, T. A. Prince, Phys. Rev. 10 (1974) 3594

[15] G.M. Garibian, L. A. Gevorgian, C. Yang, Nucl. Instr. and Meth. in Phys. Res., 125 (1975) 133.

[16] I. Gavrilenko, ATLAS Internal Note, ATLAS-INDET-No-165 (1997).

[17] ATLAS Detector and Physics Performance Technical Design Report, CERN/LHCC/99-15, ATLAS TDR 15 (1999), p. 561-618.

[18] Proceedings of the workshop on standard model physics (and more) at the LHC, G. Altarelli and M.L. Mangano editors, CERN 2000-004, p 329-333